RSC Advances

PAPER

View Article Online
View Journal | View Issue

Check for updates

Cite this: *RSC Adv.*, 2017, 7, 39279

Bis-isoquinolinium and bis-pyridinium acetylcholinesterase inhibitors: *in vitro* screening of probes for novel selective insecticides†

Veronika Hrabcova,[ab] Jan Korabecny,[bc] Brigita Manyova,[bd] Lenka Matouskova,[bd] Tomas Kucera,[b] Rafael Dolezal,[ac] Kamil Musilek,[abc] Lukas Gorecki,[bc] Eugenie Nepovimova,[bc] Kamil Kuca[abc] and Daniel Jun *[bc]

Received 24th May 2017
Accepted 3rd July 2017

DOI: 10.1039/c7ra05838a

rsc.li/rsc-advances

Insects have a huge impact on quality of life around the world. They play roles in transmitting diseases, crop-destruction, and as residential pests. Their increased resistance to the existing pesticides and the toxicity of carbamates (CA) and organophosphates (OP) has led to the development of new environmentally safe insecticides. In our study, thirty different bis-isoquinolinium and bis-pyridinium acetylcholinesterase inhibitors were tested as candidates for potential new selective pesticides. Our compounds were evaluated *in vitro* on insect acetylcholinesterase (AChE) from *Musca domestica* and human erythrocyte AChE using the modified Ellman's method. The values of IC_{50} were compared and expressed *via* a selectivity index (SI) towards the insect enzyme. **K299**, **K416**, and **K423** provided a high SI and seem to be suitable as new lead structures of novel selective anticholinesterase insecticides. Docking studies further provided the rational background uncovering the disparities in the ligand–enzyme binding modes for each AChE enzyme. *In vitro* assessments as well as docking studies highlighted **K299** and **K416** as suitable candidates for lead structures of novel pesticides. However, further evaluation is needed to confirm this statement.

Introduction

Vector-borne diseases are among the major causes of illness and death in many tropical and subtropical countries.[1] In 2015, 214 million new cases of malaria, transmitted by *Anopheles gambiae*, globally occurred, and the disease led to 438, 000 deaths.[2] Dengue fever as well as Zika virus disease is transmitted by another mosquito species, *Aedes aegypti*. Currently, Zika virus infections indicate rapid geographic expansion.[3] Worldwide present bed bugs (*Cimex lectularius*) feed on human blood and cause mental stress, acute discomfort, and social stigma.[4] Finally, soybean aphids (*Aphis glycines*) cost US farmers more than 1 billion dollars in yield losses and the purchase and application of insecticides, hampering the production of biodiesel from soybean oil.[5] All the problems caused by crop-destroying, disease-carrying, and residential insects require urgent solutions.[6]

Carbamates (CA) and organophosphates (OP) are examples of pesticides that inhibit cholinesterases, which are commonly used for insect control.[7–9] Acetylcholinesterase (AChE; EC 3.1.1.7) is a serine esterase in the α/β hydrolase-fold enzyme family.[10] The function of AChE is to terminate neurotransmission by rapidly hydrolyzing acetylcholine (ACh) at the cholinergic synapses and neuromuscular junctions of most invertebrates and vertebrates.[7,11–13] The active site of the enzyme is located at the bottom of a deep and narrow gorge, containing a serine residue in a catalytic triad.[7,13] Current anticholinesterase insecticides work through covalent modification of serine at the active site of an enzyme, thus disabling its catalytic function and incapacitating insects.[7–9]

Due to the long-lasting consumption of pesticides, more and more insect species have developed resistance.[14–16] This resistance has been claimed to be due to three different mechanisms: reduction in insecticide sensitivity of target enzymes, decrease in insecticide penetration into the insect body, and increase in detoxification activities.[17] On the other hand, acute pesticide poisonings (APPs) are responsible for significant morbidity and mortality worldwide, particularly in developing countries.[18] Estimates of the total number of poisonings are quite variable, depending on the period and author. Despite some limitations, a total number of APPs in the range from 250 000 to 500 000 were

[a]*University Hradec Kralove, Faculty of Science, Department of Biology, Rokitanskeho 62, 50003 Hradec Kralove, Czech Republic*

[b]*University of Defence, Faculty of Military Health Sciences, Department of Toxicology and Military Pharmacy, Trebesska 1575, 500 01 Hradec Kralove, Czech Republic. E-mail: daniel.jun@unob.cz; Tel: +420 973 255 193*

[c]*University Hospital, Biomedical Research Centre, Sokolska 581, 500 05 Hradec Kralove, Czech Republic*

[d]*Charles University, Faculty of Pharmacy, Department of Pharmacology and Toxicology, Akademika Heyrovskeho 1203, 500 05 Hradec Kralove, Czech Republic*

† Electronic supplementary information (ESI) available. See DOI: 10.1039/c7ra05838a

estimated yearly with 3000–30 000 fatalities.[19] Due to the increasing insect resistance to pesticides, off-target toxicity, and several epidemic situations of insect-transmitted diseases, the development of new selective insecticides is needed.

Our aim was to screen selected recently reported AChE inhibitors from our in-house library[20–22] and find out if any of them provided selectivity to insect AChE. These selective inhibitors could be used as new structure leads for further research. Approximately thirty different symmetrical bis-quaternary AChE inhibitors, namely bis-isoquinolinium and bis-pyridinium salts, were evaluated as new pesticide candidates, and the selectivity of these compounds was determined. Due to the fact that *Musca domestica* has just one type of AChE responsible for cholinergic function,[11] it has been chosen as a suitable source of insect enzyme. Finally, *in silico* studies were carried out to justify the results obtained from the *in vitro* assessment. Predictive binding poses of the selected ligands are shown in the cavity of greenbug AChE (*Schizaphis graminum*, *Sg*AChE; enzyme structurally related to *Anopheles gambiae* and/or *Aedes aegypti* AChE) to validate our hypothesis for the compounds under study.

Results and discussion

Biological assay

Herein, thirty different symmetrical bis-quaternary AChE inhibitors were assayed for their selectivity using the modified spectrophotometric method described by Ellman *et al.*[23–25] The validity of our protocol has been verified on the anti-Alzheimer's disease drug tacrine, a well-known AChE inhibitor (data not shown in the table).[26,27] *Musca domestica* was used as a suitable source of the insect AChE. *Anopheles gambiae*, a mosquito that transmits malaria, has two types of AChE: paralogous AChE (AP-AChE) to the *Drosophila melanogaster* gene, which is responsible for cholinergic function in mosquito, and orthologous AChE (AO-AChE), which plays a crucial role in the process of reproduction. On the other hand, *Musca domestica*, which belongs to the true fly species, has only one type of AChE, AO-AChE, in particular.[6]

The compounds chosen for selectivity screening can be divided into two groups based on their structural features. All these structures have been recently reported as potential candidates for the treatment for AD or myasthenia gravis.[20–22] The first group consisted of symmetrical bis-pyridinium compounds (see Fig. 1), which was selected based on the linker length and its previously reported inhibition effect. The IC_{50} values are listed in Table 1.

Initially, **K366** was the non-substituted bis-pyridinium salt connected with a naphthylene linkage. The IC_{50} value of **K366** was in the micromolar range for both types of AChE. However, selectivity towards *Md*AChE was very low. **K364** and **K365** are (*E*) and (*Z*) non-substituted bispyridinium isomers with a but-(2*E*)-en-1,4-diyl linker, respectively. They displayed no inhibition effect in the tested concentration scale. The aromatic linkage displayed a promising inhibitory effect, opposite to the linker with a double bond. On the other hand, the substitution at the *para* position of bis-pyridinium inhibitors with the but-(2*E*)-en-1,4-diyl linker diminished the inhibitory ability.

para-Substituted bispyridinium inhibitors (**K420–K435**) provided a very wide inhibition effect based on the used substituent. Lipophilic moieties, such as aliphatic functional groups (**K420–K422**), resulted in poor inhibition as compared to the compounds with an aromatic ring. Among the aromatic functional groups (**K423–K426**), a phenyl-bearing compound (**K423**) was found to be the best inhibitor of *Md*AChE, having an IC_{50} in the nanomolar range with a SI value of 7.058, which was superior to that of the benzyl compound (**K424**) or the 3-phenylpropyl compound (**K425**). The latter compound exerted no or very low inhibition potency to *Md*AChE in the given concentration scale. The results showed that only **K423**, bearing a phenyl ring directly attached to the pyridinium moiety, was able to inhibit *Md*AChE, whereas chain elongation between these two moieties (**K424** and **K425**) resulted in the loss of activity. On the other hand, a 4-nitrobenzyl compound (**K426**) showed inhibition in the micromolar scale although its selectivity towards *Md*AChE was very low. Compounds (**K427–K435**) containing hydrophilic functional groups also showed apparent differences in their inhibitory ability. Among them, 3-hydroxypropyl (**K429**), *N*,*N*-dimethylamino (**K430**), and 4-carbonitrile compound (**K435**) were superior to other hydroxyl- (**K427**, **K428**) or carbonyl-containing compounds (**K431–K434**), possessing IC_{50} values in the micromolar range. Among the hydroxyl-containing compounds (**K427–K429**), no clear SAR can be drawn since only **K429** was able to inhibit *Md*AChE. However, the SI values towards *Md*AChE were negligible for all of them. Although **K429**, **K430**, and **K435** were the best hydrophilic compounds, their inhibitory ability towards *Md*AChE still decreased by two orders of magnitude as compared to that of the phenyl analogue **K423**.

The second subset of compounds consisted of bis-isoquinolinium derivatives bearing various linkers (see Fig. 2). The bis-isoquinolinium derivatives (**K291–K299**, **K302**, and **K412–K419**) were the most potent inhibitors in our study; only three of them (**K291**, **K293**, and **K413**) did not inhibit human and insect AChEs in the tested concentration range. This is probably caused by the presence of the isoquinoline heterocycle in them, which exhibits stronger stabilization *via* π–π or cation–π interaction to the catalytic active site (CAS) and peripheral anionic site (PAS) as compared to the bis-pyridinium compounds.[21] Moreover, the used linkage and its length markedly influenced the inhibitory ability of bis-isoquinolinium compounds.[21,28] Among the compounds with an aliphatic linker (**K291–K299**, **K302**, and **K412–K415**), those with nine and twelve methylene units (**K299** and **K302**) were found to be the best inhibitors of *Md*AChE, achieving an IC_{50} value in the nanomolar range. **K296**, bearing six methylene linkers, inhibited *Md*AChE in the micromolar range with a low selectivity profile towards both AChEs. Furthermore, compounds bearing shorter linkers (one and three methylenes) were found to be inefficient for both enzymes, which was in agreement with previously obtained results.[22,28] The presence of an oxygen heteroatom (**K412** and **K413**) or a double bond (**K414** and **K415**) in the linker did not yield higher affinity. In this case, the IC_{50} values lay in the micromolar range, and low selectivity towards *Md*AChE was observed. The linkage length of these

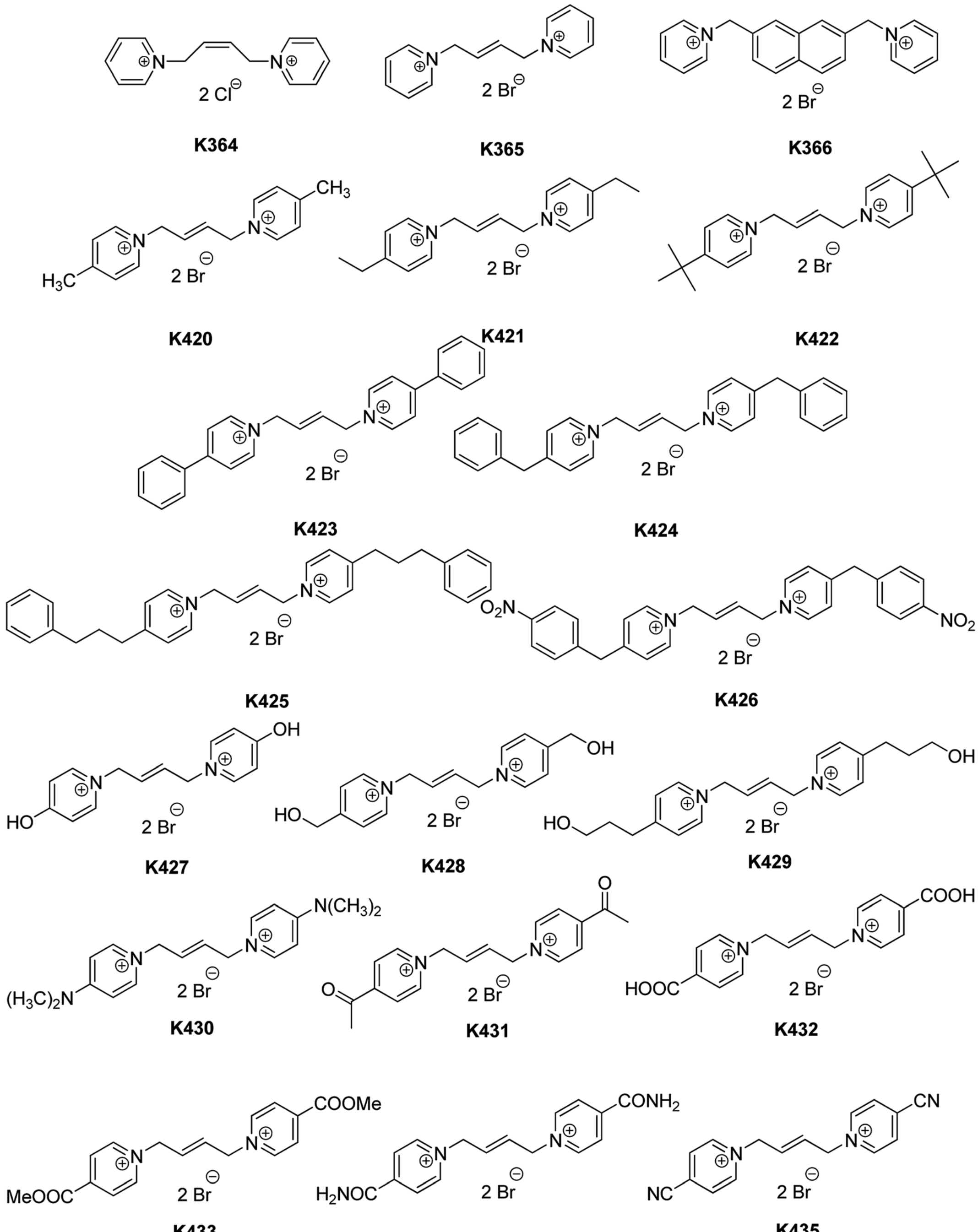

Fig. 1 Structures of the evaluated standards and bis-pyridinium compounds (non-substituted and *p*-substituted).

compounds was four methylene units, which correlated well with the result obtained for **K296**.

Among bis-isoquinolinium salts bearing aromatic linkers (**K416–K419**), naphthylene-linked dimers (**K419**) were more potent as compared to xylene-linked dimers (**K416–K419**). **K419** inhibited *Md*AChE in the nanomolar range, but with low selectivity. On the other hand, **K416–K418** revealed high selectivity for *Md*AChE over *h*AChE. In this regard, **K416** possessed the highest SI value of 12.185, and the second top-ranked compound **K417** had a three-fold lower SI value of 4.789. However, the most promising compounds in terms of the IC_{50} values were **K299**, **K302**, and **K419**, achieving IC_{50} values in the nanomolar range.

A group of four insecticides (pyrethroids (PY), carbamates (CA), organophosphates (OP), and organochlorines (OC)) has currently been recommended by WHO pesticide evaluation scheme (WHOPES) for controlling vector-borne disease such as malaria.[29] Compared to organophosphates, the carbamate insecticides probably represent a better option because they act as pseudo-irreversible AChE inhibitors with lower dermal

Table 1 The IC_{50} values of the evaluated compounds

Compound	IC_{50} *h*AChE ± SEM[a] (μM)	IC_{50} *Md*AChE ± SEM[a] (μM)	SI for *Md*AChE
Propoxur	2.094 ± 0.040[b]	0.152[c]	13.78
Bendiocarb	0.359 ± 0.016[b]	0.058[c]	6.19
Compound **1**	0.201 ± 0.019[b]	0.181[c]	1.11
Compound **7**	20.68 ± 9.509[b]	0.051[c]	405
Compound **8**	247.4 ± 106.8[b]	0.654[c]	378
K291	>1000	>1000	—
K293	>1000	>1000	—
K296	0.881 ± 0.322	2.77 ± 0.08	0.318
K299	0.138 ± 0.008	0.0226 ± 0.0006	6.093
K302	0.0697 ± 0.0032	0.036 ± 0.001	1.936
K364	>1000	>1000	—
K365	>1000	>1000	—
K366	8.01 ± 1.30	14.1 ± 1.5	0.568
K412	5.10 ± 0.39	7.40 ± 0.39	0.690
K413	>1000	693 ± 59	—
K414	15.78 ± 1.12	17.6 ± 2.1	0.897
K415	38.7 ± 4.4	112 ± 11	0.346
K416	267 ± 11	21.9 ± 4.7	12.185
K417	8.59 ± 0.86	1.79 ± 0.12	4.789
K418	5.87 ± 0.49	5.56 ± 0.49	1.056
K419	0.214 ± 0.011	0.228 ± 0.009	0.936
K420	>1000	>1000	—
K421	>1000	>1000	—
K422	>1000	>1000	—
K423	4.93 ± 3.61	0.699 ± 0.089	7.058
K424	4.09 ± 1.01	>1000	—
K425	0.0554 ± 0.0029	>1000	—
K426	5.19 ± 0.56	20.7 ± 2.8	0.251
K427	>1000	>1000	—
K428	>1000	>1000	—
K429	31.5 ± 2.0	107 ± 15	0.294
K430	1.05 ± 0.06	4.14 ± 0.23	0.253
K431	>1000	>1000	—
K432	>1000	>1000	—
K433	>1000	>1000	—
K434	>1000	>1000	—
K435	37.3 ± 3.3	103 ± 11	0.362

[a] The IC_{50} values are derived from triplicate and selectivity indexes (SI) were calculated as a ratio of IC_{50} value for *h*AChE/IC_{50} value for *Md*AChE. [b] Data were obtained from ref. 30. [c] Data were obtained from ref. 31.

toxicity. Moreover, two approved CA for insecticide-treated nets (ITN) are propoxur and bendiocarb, usually combined with PY. The IC_{50} value of *h*AChE for bendiocarb was found to be in the submicromolar range (IC_{50} 0.359 μM), which was one order of magnitude lower than that of propoxur (2.094 μM).[30] Based on the reported data, the SI for both of these compounds were calculated (propoxur SI 13.78 and bendiocarb 6.19).[30,31] The highlighted compounds in our screening study in terms of SI are **K299**, **K416**, and **K423**. All these analogues resemble the SI values of the approved CA. **K416** with a SI of 12.19 is superior to **K423** (SI 7.06) and to **K299** (SI 6.09). In terms of *Md*AChE inhibition potency, **K299** was able to block the enzyme activity in the same range as bendiocarb. **K423** had a comparable effect with propoxur. However, these data need to be taken with precaution since bendiocarb and propoxur presumably exert different modes of AChE inhibition.

Due to the fact that increase in resistance affects all major malaria vector species over all four recommended classes of insecticides,[2,31] the development of new insecticides is currently a hot issue. Among the insecticides targeting AChE, a novel class of methylcarbamate hybrids has been developed.[32,33] In this family, the most potent inhibitors were *meta*-substituted to the phenyl ring (compound **1**) and possessed an IC_{50} value in the nanomolar range with low selectivity towards *Md*AChE.[30,33] Compared to those of our highlighted inhibitors (**K299**, **K302**, and **K419**), their inhibitory effect and selectivity index were very similar. On the other hand, the *ortho*-substituted carbamate derivatives (compounds **7** and **8**), which possessed higher values of IC_{50}, *h*AChE, exhibited up to 350-fold selectivity, which significantly exceeded that of our most of the selective compounds (**K299**, **K416**, and **K423**) in this study. Recently, Pang *et al.* have described thiol-reactive compounds, which interfere with free cysteine in PAS of *Ag*AChE; *h*AChE has no such free cysteine.[9] These experimental thiol-compounds inhibited >95% of *Ag*AChE activity after a 1 h exposure at 6 μM. Under this condition, *h*AChE activity remained unchanged.[8] This suggested that inhibitors that bind to CAS and concomitantly target free cysteine may lead to highly selective insecticides. In this regard, our screened compounds are dual-binding site inhibitors; thus, in some ways, they follow the innovative Pang's dual binding site strategy.

Moreover, it was described that bis-pyridinium compounds bearing a polymethylene linker of up to four carbons did not inhibit the response of the nicotinic ACh receptor.[34] Furthermore, a representative compound of bis-isoquinolinium salts was also evaluated for its nicotinic effect, and no inhibitory ability was confirmed.[35] Therefore, we do not speculate any inhibitory effect of our most promising compounds (**K299**, **K416**, and **K423**) on the nicotinic ACh receptors.

Docking studies

To explain the reasons for varied potencies between *h*AChE and *Md*AChE inhibition, several ligands were docked into their active sites as these enzymes were involved in the biological assay. In this context, we followed our previously described protocol.[36–39] Moreover, the prediction of the ligand anchored onto the cavity of greenbug AChE (*Schizaphis graminum*, *Sg*AChE) was carried out. The rationale for selection of this enzyme is structural similarity to *Anopheles gambiae* AChE.[13] Moreover, the structure of *Sg*AChE is freely available from the RCSB Protein Data Bank as a 3D theoretical model (PDB ID: 2HCP). The crystal structure of *h*AChE (PDB ID: 4EY7) with the well-known Alzheimer's disease drug donepezil was used as the template receptor for docking.[32,40,41] Donepezil, likewise the intended ligands used in this study, is a dual-binder, *i.e.* a compound capable of simultaneously interacting with both anionic sites of AChE. *Md*AChE enzyme is not freely available from the RCSB Protein Data Bank; hence, this enzyme has been created based on the homology modeling technique and further validated before performing the *in silico* calculations (see the

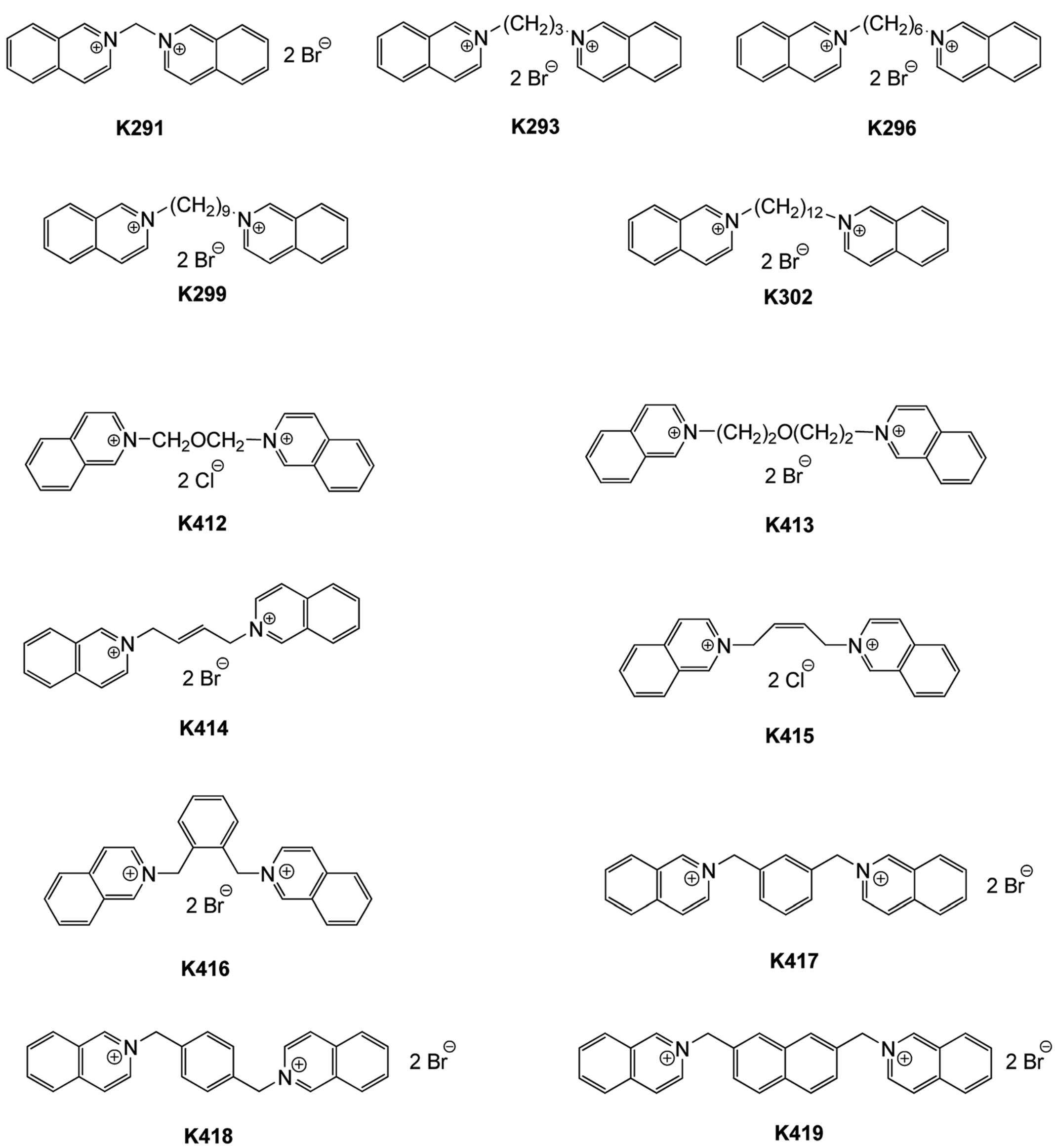

Fig. 2 Structures of the evaluated bis-isoquinolinium compounds with aliphatic and aromatic linkers.

Experimental section). Based on the selectivity and activity profiles, we have chosen **K299**, being the most potent inhibitor of *Md*AChE from the family of bis-isoquinolinium salts, **K416**, having the highest selectivity ratio index for *Md*AChE under this study, **K423**, the highlighted *Md*AChE inhibitor from bis-pyridinium salts, and **K425**, as the highly effective *h*AChE binder with no activity towards MdAChE in the tested concentration scale.

Initially, **K299** revealed a dual-binding site character in all three models of AChE (Fig. 3), but with several divergences that might explain different enzyme affinity.[22] Regarding the *h*AChE enzyme (Fig. 3A and B), the proximal isoquinoline heterocyclic core is engaged in parallel π–π/cation–π interactions with Tyr337 (3.8 Å), T-shaped π–π/cation–π interaction with Trp86 (3.5 Å), and π–π stacking with Phe338 (3.7 Å), whereas the distal isoquinoline moiety is sandwiched between Trp286 (3.6 Å) and Tyr124 (4.1 Å) *via* π–π and/or cation–π stacking. The linker combining both isoquinolines is responsible for weak van der Waals contact to Phe297 and Tyr341. Ser203 from the catalytic triad displayed a hydrophobic interaction to **K299**. On the contrary, His447 demonstrated unfavorable positive–positive repulsion to charged nitrogen from the proximal isoquinoline moiety. The **K299**-*Md*AChE (Fig. 3C and D) complex is somewhat different from the **K299**-*h*AChE ternary complex.

The overall arrangement in the **K299**-*Md*AChE complex placed the ligand in proximity of Tyr151, making this amino acid a cornerstone for contacting both isoquinolines as well as nine-methylene linker *via* either π–π/cation–π or hydrophobic interactions. Several other important amino acid residues provided contact to **K299**. In this case, no catalytic triad residue showed contact to **K299**. The last model **K299**-*Sg*AChE in some way combines positive features of the previously mentioned **K299**-*h*AChE and **K299**-*Md*AChE ternary complexes. Tyr335 (*Sg*AChE) is equal to Tyr151 (*Md*AChE) and hence fulfils the role of the central amino acid in which proximity **K299** lies. The distal isoquinoline core is sandwiched between Trp283 (3.6 Å) and Tyr124 (4.0 Å).

In terms of the balanced selectivity and potency prediction using docking studies, all the abovementioned observations indicate that **K299** can be the lead candidate in the search for a novel pesticide. However, further evaluation is necessarily needed to confirm this statement.

Continuing with the bis-isoquinolinium subset, the compound **K416** (Fig. 4) was preferably selected for docking simulation instead of other aromatically linked bis-isoquinolinium salts (**K417**, **K418**, and **K419**) based on the highest selectivity profile towards *Md*AChE. It is well-known that introduction of a flexible linker in combination with an aromatic moiety leads to activity enhancement.[32,42] This is in accordance ith the aromatic residue-abundant character of the mid-gorge region of the AChE enzyme. Indeed, this might be the case for some derivatives from the family of aromatically linked bis-isoquinolinium salts. However, hybrids used in this study combined only the short methylene chain with the aromatic part, which in general did not reach the inhibition potency of alkyl-tethered bis-isoquinolinium salts. This is presumably caused by the insufficient length of aromatically linked bis-isoquinolinium salts between the catalytic anionic site (CAS) moiety and the peripheral anionic site (PAS) binder, *i.e.* between both isoquinoline cores. The distance between these regions for an ideal inhibitor was found to be around 20 Å.[43] Apart from all these, **K416** is specific as compared to other inhibitors inspected in this study because it contains an *o*-disubstituted xylylene moiety. This liability is plausibly responsible for less linear properties in **K416** as compared to those in other aromatically linked inhibitors (**K417**, **K418**, and **K419**), thus preserving steric rigidity leading to specific interactions and discrepancies in the binding sites of each AChE enzyme. Upon closer observation of the 3D complex of **K416**-*h*AChE (Fig. 4A and B), it was evident that the distal isoquinoline core was not able to establish favorable π–π/cation–π contact with Trp286, a crucial PAS amino acid residue. This amino acid residue is only involved in very weak hydrophobic contact. On the contrary, the proximal isoquinoline moiety is engaged in face-to-face π–π/cation–π interaction with Tyr341 (3.8 Å). This amino acid residue is also implicated in distorted π–π stacking with the connecting *o*-xylylene moiety with the distance of 3.8 Å. At the opposite site, deep in the gorge of *h*AChE, proximal isoquinoline can be found, forming parallel π–π contact with Trp86 (3.9 Å). No direct interaction can be observed between **K416** and the catalytic triad residues of hAChE. In contrast, **K416** revealed edge-to-edge ligand anchoring supported by parallel π–π interactions with Tyr151 (3.6 Å) and a sandwich orientation to Tyr447 (4.0 Å) and Trp163 (3.8 Å) in the PAS and CAS regions of *Md*AChE, respectively. Additionally, His557 from the catalytic triad furnished plausible hydrophobic contact with **K416**. Several other interactions can be found as well, *e.g.* σ–π contact between the distal isoquinoline heterocycle and Thr232, alkyl–π interaction with Met231, van der Waals interactions with Tyr407, Trp549, and Glu160, and many others. All the amino acid residues encompassing the **K416** in the cavity of *Md*AChE are highlighted in Fig. 4(C and D). These findings justify the high potency and selectivity of **K416** for *Md*AChE over *h*AChE. The investigation of the predictive model of **K416** in *Sg*AChE (Fig. 4E and F) is closely related to that of the **K299**-*Sg*AChE complex with Tyr335 networking both isoquinolines. In this case, a plethora of attractive interactions can be found such as plausible cation–π interactions with Tyr124, Asp75, and Tyr331. The catalytic triad seems to stand aside of enzyme–ligand anchoring.

Via probing **K423**, the most potent and selective *Md*AChE binder from the bis-pyridinium family containing a but-(2*E*)-en-1,4-diyl linker, some structure diversity in the specific AChE active sites can be concluded. Considering the **K423**-*h*AChE complex (Fig. 5A and B), **K423** furnished a typical dual-binding site pattern spanning the cavity gorge from the entrance to the bottom of the deep gorge. Every aromatic part of the ligand revealed face-to-face π–π and/or cation–π interactions with its amino acid counterpart proximally to the enzyme center in the order Trp286 (3.7 Å), Tyr341 (4.0 Å), Tyr337 (3.7 Å), and Trp86 (4.0 Å). Interestingly, all the catalytic triad residues are connected through hydrophobic interaction to **K423**. In contrast to *h*AChE, **K423** mimics a similar spatial orientation in *Md*AChE (Fig. 5C and D), extending from the rim to underneath the gorge. Similarly, each aromatic part of the ligand displayed

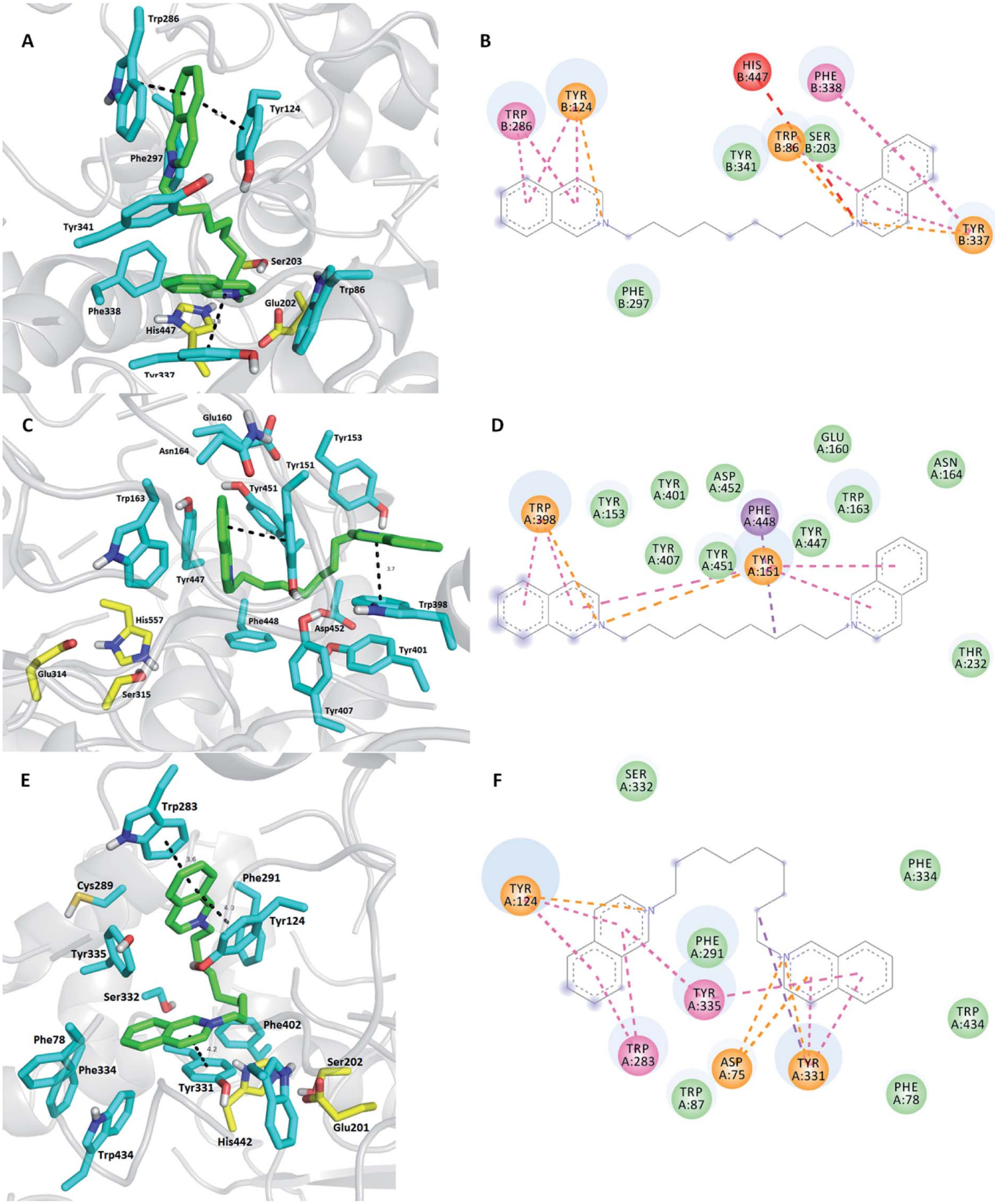

Fig. 3 Superimposition of **K299** at *h*AChE, *Md*AChE, and *Sg*AChE active sites displayed in figures (A, C, and E), respectively, as 3D ternary complexes. 2D diagrams for **K299** in *h*AChE, *Md*AChE, and *Sg*AChE are shown in figures (B, D, and F), respectively. The ligand is rendered as green carbon atoms, the amino acid residues involved in the enzyme–ligand interaction are shown as blue carbon atoms, and the catalytic triad is portrayed in yellow (A, C, and E). The rest of the enzyme is depicted as a grey cartoon (A, C, and E). 2D diagrams (figures B, D, and F) were created with Discovery Studio 2016 Client, whereas 3D figures were generated using PyMol 1.5.0.4 (The PyMOL Molecular Graphics System, Version 1.5.0.4 Schrödinger, LLC, Mannheim, Germany). Legend for 2D diagrams: blue spots on the ligand's carbons designate areas of hydrophobic interaction; orange dashes/residues represent cation–π interactions; pink dashes/residues show π–π stacked or T-shaped contacts; green residues delineate van der Waals contacts; red dashes/residues are for unfavorable positive–positive repulsion.

favorable π–π and/or cation–π contacts with aromatic amino acid residues delineating the cavity enzyme. Stronger affinity of **K423** to *Md*AChE over *h*AChE might be provided by the web of several cation π interactions, as illustrated in Fig. 4D. The model of **K423**-*Sg*AChE (Fig. 5E and F) gave the worst fit to the active site and thus could be considered as the potential

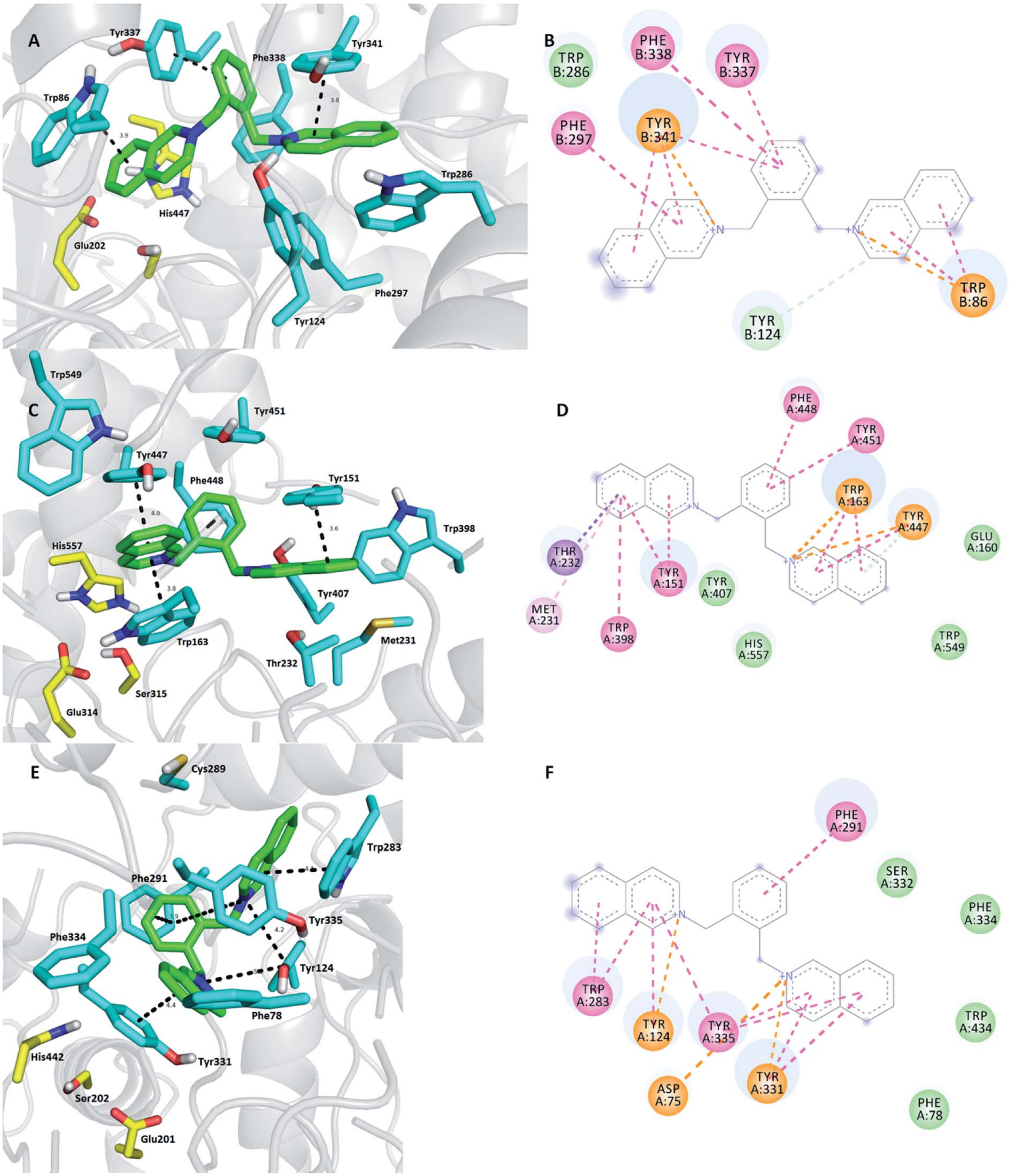

Fig. 4 Superimposition of **K416** at *h*AChE, *Md*AChE, and *Sg*AChE active sites displayed in figures (A, C, and E), respectively, as 3D ternary complexes. 2D diagrams for **K416** in *h*AChE, *Md*AChE, and *Sg*AChE are shown in figures (B, D, and F), respectively. The ligand is rendered as green carbon atoms, the amino acid residues involved in the enzyme–ligand interaction are shown as blue carbon atoms, and the catalytic triad is portrayed in yellow (A, C, and E). The rest of the enzyme is depicted as a grey cartoon (A, C, and E). 2D diagrams (figures B, D, and F) were created with Discovery Studio 2016 Client, whereas 3D figures were generated using PyMol 1.5.0.4 (The PyMOL Molecular Graphics System, Version 1.5.0.4 Schrödinger, LLC, Mannheim, Germany). Legend for 2D diagrams: blue spots on the ligand's carbons designate areas of hydrophobic interaction; orange dashes/residues represent cation–π interactions; pink dashes/residues show π–π stacked or T-shaped contacts; green residues delineate van der Waals contacts; red dashes/residues are for unfavorable positive–positive repulsion.

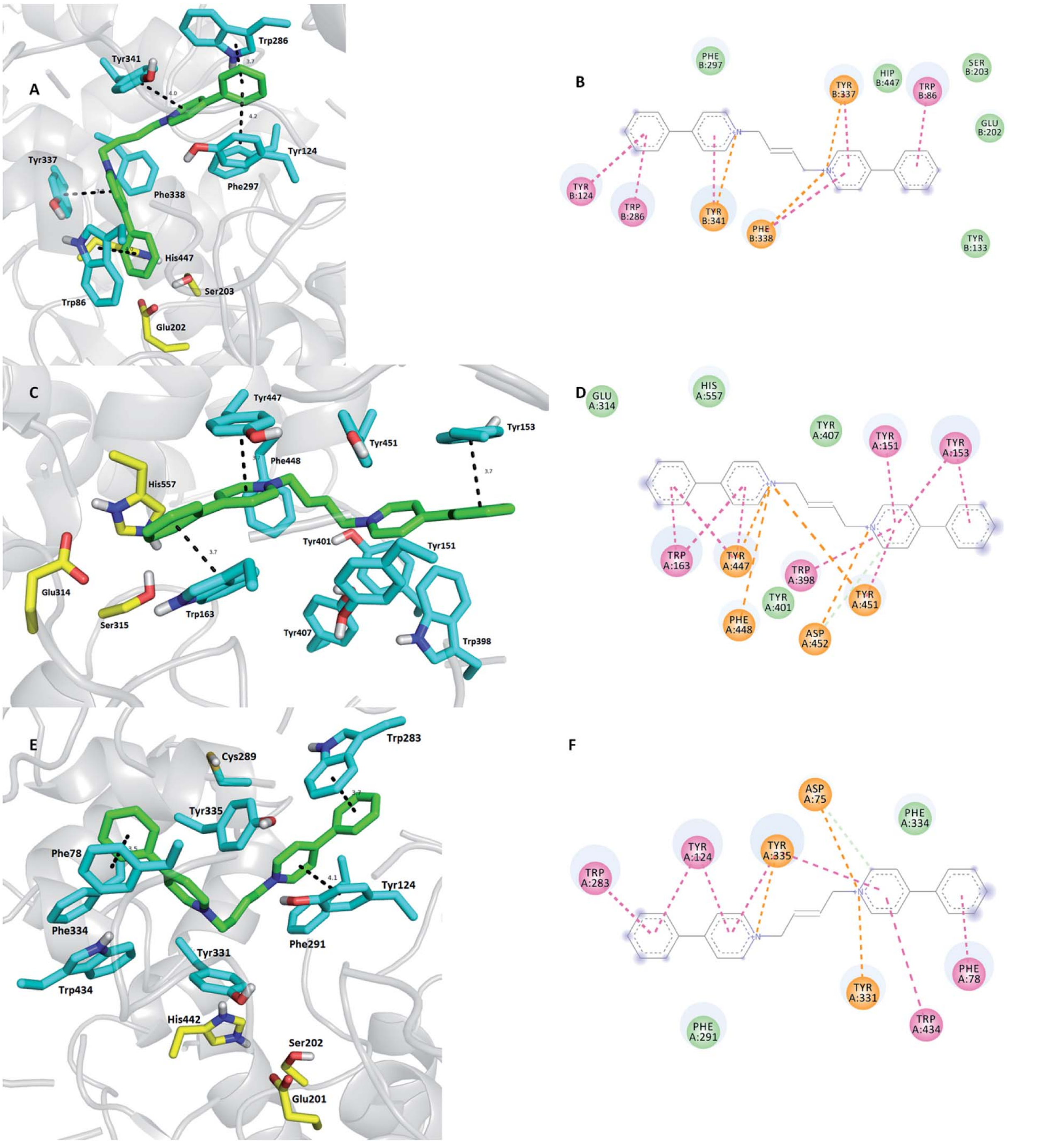

Fig. 5 Superimposition of **K423** at *h*AChE, *Md*AChE, and *Sg*AChE active sites displayed in figures (A, C, and E), respectively, as 3D ternary complexes. 2D diagrams for **K423** in *h*AChE, *Md*AChE, and *Sg*AChE are shown in figures (B, D, and F), respectively. The ligand is rendered as green carbon atoms, the amino acid residues involved in the enzyme–ligand interaction are shown as blue carbon atoms and the catalytic triad is portrayed in yellow (A, C, and E). The rest of the enzyme is depicted as a grey cartoon (A, C, and E). 2D diagrams (figures B, D, and F) were created with Discovery Studio 2016 Client, whereas 3D figures were generated using PyMol 1.5.0.4 (The PyMOL Molecular Graphics System, Version 1.5.0.4 Schrödinger, LLC, Mannheim, Germany). Legend for 2D diagrams: blue spots on the ligand's carbons designate areas of hydrophobic interaction; orange dashes/residues represent cation–π interactions; pink dashes/residues show π–π stacked or T-shaped contacts; green residues delineate van der Waals contacts; red dashes/residues are for unfavorable positive–positive repulsion.

pesticide with the lowest interest in this study. This is mainly speculated to be due to the unbeneficial occupation of the cavity of *Sg*AChE where some face-to-face π–π stacking is missing and also the density of cation–π interactions is not so high.

Lastly, our *in silico* study disclosed **K425** as the ligand with no activity towards *Md*AChE and high affinity to the *h*AChE enzyme in the tested concentration scale (Fig. 6).[28] Taking into account all the findings, no clear results or SAR data can be drawn based on

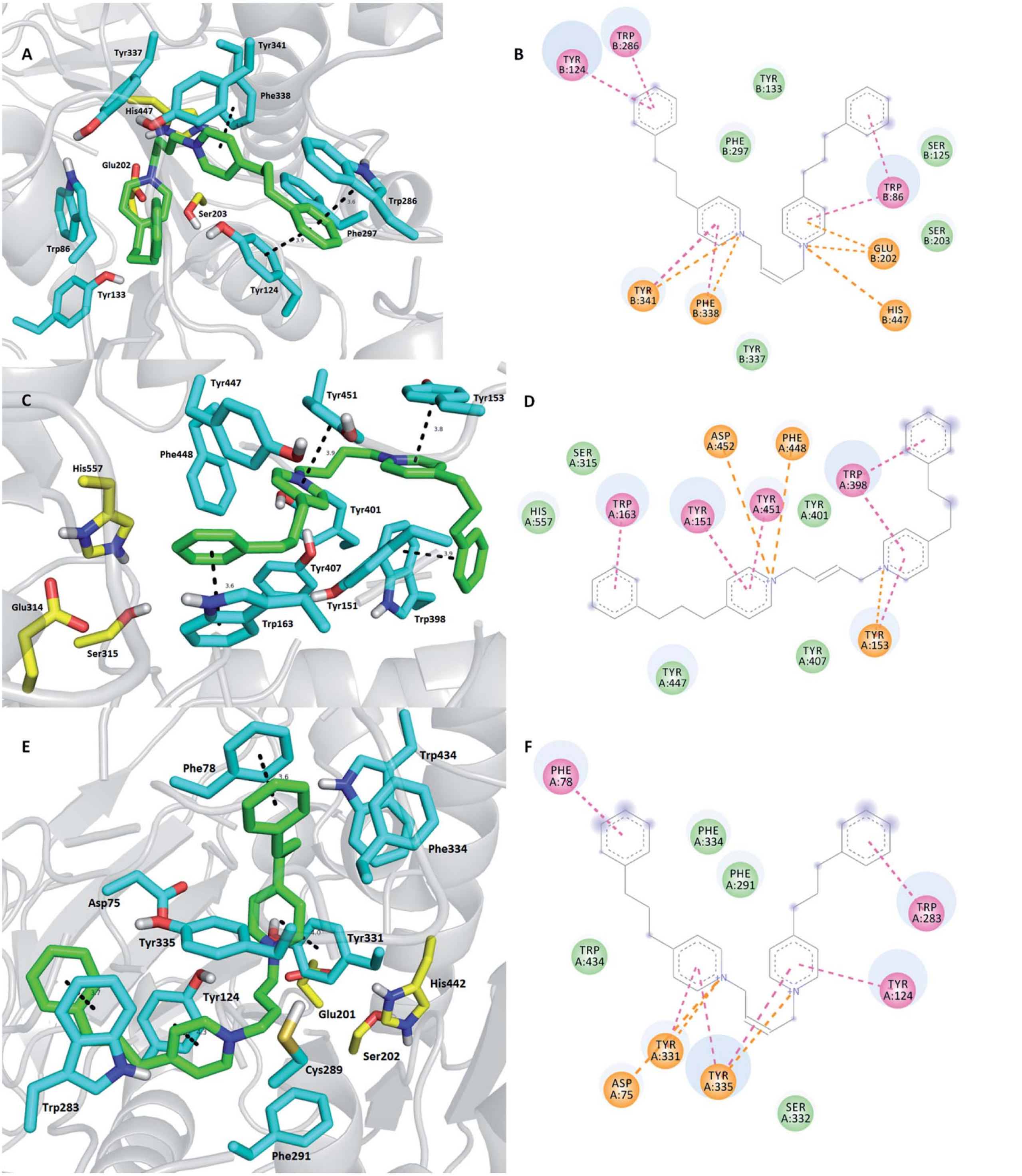

Fig. 6 Superimposition of **K425** at *h*AChE, *Md*AChE, and *Sg*AChE active sites displayed in figures (A, C, and E), respectively, as 3D ternary complexes. 2D diagrams for **K425** in *h*AChE, *Md*AChE, and *Sg*AChE are shown in figures (B, D, and F), respectively. The ligand is rendered as green carbon atoms, the amino acid residues involved in the enzyme–ligand interaction are shown as blue carbon atoms and the catalytic triad is portrayed in yellow (A, C, and E). The rest of the enzyme is depicted as a grey cartoon (A, C, and E). 2D diagrams (figures B, D, and F) were created with Discovery Studio 2016 Client, whereas 3D figures were generated using PyMol 1.5.0.4 (The PyMOL Molecular Graphics System, Version 1.5.0.4 Schrödinger, LLC, Mannheim, Germany). Legend for 2D diagrams: blue spots on the ligand's carbons designate areas of hydrophobic interaction; orange dashes/residues represent cation–π interactions; pink dashes/residues show π–π stacked or T-shaped contacts; green residues delineate van der Waals contacts; red dashes/residues are for unfavorable positive–positive repulsion.

the molecular level of the enzyme–ligand interaction. This is indeed true for all three cases of **K425** *h*AChE, **K425** *Md*AChE, and **K425** *Sg*AChE where no clear differences can be observed in the ligand lodging. Presumably, more definite results might be generated *via* molecular dynamics or Monte Carlo methods; however, these techniques are beyond the scope of this study.[44,45] The docking score calculated by the Vina score (hybrid scoring function combining empirical and knowledge-based scoring) for **K425** *h*AChE, **K425** *Md*AChE, and **K425** *Sg*AChE complexes was -12.7 kcal mol^{-1}, -12.4 kcal mol^{-1}, and -13.0 kcal mol^{-1}, respectively, which slightly correlated with the obtained *in vitro* results. Moreover, the energetic balance obtained for the **K425** *Sg*AChE complex does not discriminate this ligand from further development as a selective pesticide. Note that further biological assays towards *Sg*AChE or related enzymes are necessarily needed to make any clear conclusion.

Conclusions

In summary, 34 compounds were evaluated for their inhibition ability to human and insect AChE. Their potency to inhibit *h*AChE and *Md*AChE was tested *in vitro*, and SI values were calculated to establish their selectivity. The most promising compounds in terms of selectivity were **K299**, **K416**, and **K423**, being more selective than the approved carbamates for controlling vector-borne disease. Consequently, the promising selectivity of these screened compounds was determined *via* docking study with *h*AChE, *Md*AChE, and *Sg*AChE. The apparent interactions of π–π or π–cationic origin were described with several discrepancies indicating the binding differences. The docking study highlighted **K299** and **K416** as the candidates for lead structures in novel pesticides. However, further evaluation is needed to confirm this proof-of-concept.

Acknowledgements

The authors would like to thank Jitka Turanova for her technical assistance. The work was financially supported by the Ministry of Health of the Czech Republic (No. 16-34390A) and by Ministry of Education, Youth and Sports of the Czech Republic (No. SV/UHK2109 and No. SV/FVZ201601). Computational resources were provided by the CESNET LM2015042 and the CERIT Scientific Cloud LM2015085, provided under the programme "Projects of Large Research, Development, and Innovations Infrastructures". The experiments were performed in compliance with the Czech legislation and institutional guidelines of the Faculty of Military Health Sciences, University of Defence. The institutional ethical committee of the Faculty of Military Health Sciences, University of Defence approved the experiment. The informed consents were obtained from all human subjects who provided the blood samples.

Notes and references

1 WHO/WHOPES, WHO Pesticides Evaluation Scheme, WHO, cited 2015 May 15, http://www.who.int/whopes/questions/en/.

2 WHO/Fact Sheet, World Malaria Report 2015, WHO, cited 2016 Sep 21, http://www.who.int/malaria/media/world-malaria-report-2015/en/.

3 WHO/Zika virus, WHO, cited 2016 Feb 3, http://www.who.int/mediacentre/factsheets/zika/en/.

4 C. Boase, Bedbugs – back from the brink, *Pestic. Outlook*, 2001, **12**(4), 159–162.

5 D. W. Ragsdale, B. P. McCornack, R. C. Venette, B. D. Potter, I. V. MacRae, E. W. Hodgson, *et al.*, Economic threshold for soybean aphid (Hemiptera: Aphididae), *J. Econ. Entomol.*, 2007, **100**(4), 1258–1267.

6 Y.-P. Pang, Chapter Six – Insect Acetylcholinesterase as a Target for Effective and Environmentally Safe Insecticides, in *Advances in Insect Physiology*, ed. E. Cohen, Academic Press, 2014, vol. 46, p. 435–494, available from: http://www.sciencedirect.com/science/article/pii/B9780124170100000069.

7 Y.-P. Pang, Novel acetylcholinesterase target site for malaria mosquito control, *PLoS One*, 2006, **1**, e58.

8 Y.-P. Pang, S. K. Singh, Y. Gao, T. L. Lassiter, R. K. Mishra, K. Y. Zhu, *et al.*, Selective and irreversible inhibitors of aphid acetylcholinesterases: steps toward human-safe insecticides, *PLoS One*, 2009, **4**(2), e4349.

9 Y.-P. Pang, Species marker for developing novel and safe pesticides, *Bioorg. Med. Chem. Lett.*, 2007, **17**(1), 197–199.

10 S. B. Walsh, T. A. Dolden, G. D. Moores, M. Kristensen, T. Lewis, A. L. Devonshire, *et al.*, Identification and characterization of mutations in housefly (Musca domestica) acetylcholinesterase involved in insecticide resistance, *Biochem. J.*, 2001, **359**(1), 175–181.

11 Y. Lu, Y. Park, X. Gao, X. Zhang, J. Yao, Y.-P. Pang, *et al.*, Cholinergic and non-cholinergic functions of two acetylcholinesterase genes revealed by gene-silencing in Tribolium castaneum, *Sci. Rep.*, 2012, **2**, 288.

12 Y. H. Kim, J. Y. Choi, Y. H. Je, Y. H. Koh and S. H. Lee, Functional analysis and molecular characterization of two acetylcholinesterases from the German cockroach, Blattella germanica, *Insect Mol. Biol.*, 2010, **19**(6), 765–776.

13 Y.-P. Pang, S. Brimijoin, D. W. Ragsdale, K. Y. Zhu and R. Suranyi, Novel and viable acetylcholinesterase target site for developing effective and environmentally safe insecticides, *Curr. Drug Targets*, 2012, **13**(4), 471–482.

14 R. N'Guessan, F. Darriet, P. Guillet, P. Carnevale, M. Traore-Lamizana, V. Corbel, *et al.*, Resistance to carbosulfan in Anopheles gambiae from Ivory Coast, based on reduced sensitivity of acetylcholinesterase, *Med. Vet. Entomol.*, 2003, **17**(1), 19–25.

15 J. M. Mutunga, T. D. Anderson, D. T. Craft, A. D. Gross, D. R. Swale, F. Tong, *et al.*, Carbamate and pyrethroid resistance in the akron strain of Anopheles gambiae, *Pestic. Biochem. Physiol.*, 2015, **121**, 116–121.

16 T. S. Awolola, O. A. Oduola, C. Strode, L. L. Koekemoer, B. Brooke and H. Ranson, Evidence of multiple pyrethroid resistance mechanisms in the malaria vector Anopheles gambiae sensu stricto from Nigeria, *Trans. R. Soc. Trop. Med. Hyg.*, 2009, **103**(11), 1139–1145.

17 D. J. Im, W. T. Kim and K. S. Boo, Purification and Partial cDNA Sequence of Acetylcholinesterase from a Korean Strain of the Housefly, Musca domestica, *J. Asia-Pac. Entomol.*, 2004, **7**(1), 81–87.

18 J. Jeyaratnam, Acute pesticide poisoning: a major global health problem, *World Health Stat. Q. Rapp. Trimest. Stat. Sanit. Mond.*, 1990, **43**(3), 139–144.

19 T. Satoh and R. C. Gupta, *Anticholinesterase Pesticides: Metabolism, Neurotoxicity, and Epidemiology*, John Wiley & Sons, 2011. p. 645.

20 K. Musilek, R. Pavlikova, J. Marek, M. Komloova, O. Holas, M. Hrabinova, *et al.*, The preparation, in vitro screening and molecular docking of symmetrical bisquaternary cholinesterase inhibitors containing a but-(2E)-en-1,4-diyl connecting linkage, *J. Enzyme Inhib. Med. Chem.*, 2011, **26**(2), 245–253.

21 K. Musilek, M. Komloova, O. Holas, M. Hrabinova, M. Pohanka, V. Dohnal, *et al.*, Preparation and in vitro screening of symmetrical bis-isoquinolinium cholinesterase inhibitors bearing various connecting linkage – Implications for early Myasthenia gravis treatment, *Eur. J. Med. Chem.*, 2011, **46**(2), 811–818.

22 K. Musilek, M. Komloova, V. Zavadova, O. Holas, M. Hrabinova, M. Pohanka, *et al.*, Preparation and in vitro screening of symmetrical bispyridinium cholinesterase inhibitors bearing different connecting linkage—initial study for Myasthenia gravis implications, *Bioorg. Med. Chem. Lett.*, 2010, **20**(5), 1763–1766.

23 G. L. Ellman, K. D. Courtney, V. Andres and R. M. Feather-Stone, A new and rapid colorimetric determination of acetylcholinesterase activity, *Biochem. Pharmacol.*, 1961, **7**, 88–95.

24 M. Pohanka, J. Z. Karasova, K. Kuca, J. Pikula, O. Holas, J. Korabecny, *et al.*, Colorimetric dipstick for assay of organophosphate pesticides and nerve agents represented by paraoxon, sarin and VX, *Talanta*, 2010, **81**(1–2), 621–624.

25 F. Worek, G. Reiter, P. Eyer and L. Szinicz, Reactivation kinetics of acetylcholinesterase from different species inhibited by highly toxic organophosphates, *Arch. Toxicol.*, 2002, **76**(9), 523–529.

26 O. Soukup, D. Jun, J. Zdarova-Karasova, J. Patocka, K. Musilek, J. Korabecny, *et al.*, A resurrection of 7-MEOTA: a comparison with tacrine, *Curr. Alzheimer Res.*, 2013, **10**(8), 893–906.

27 F. Zemek, L. Drtinova, E. Nepovimova, V. Sepsova, J. Korabecny, J. Klimes, *et al.*, Outcomes of Alzheimer's disease therapy with acetylcholinesterase inhibitors and memantine, *Expert Opin. Drug Saf.*, 2014, **13**(6), 759–774.

28 M. Komloova, K. Musilek, A. Horova, O. Holas, V. Dohnal, F. Gunn-Moore, *et al.*, Preparation, in vitro screening and molecular modelling of symmetrical bis-quinolinium cholinesterase inhibitors—implications for early Myasthenia gravis treatment, *Bioorg. Med. Chem. Lett.*, 2011, **21**(8), 2505–2509.

29 WHO/WHO Pesticide Evaluation Scheme, "WHOPES", WHO, cited 2016 Sep 21, http://www.who.int/whopes/en/.

30 Y. Jiang, D. Swale, P. R. Carlier, J. A. Hartsel, M. Ma, F. Ekström, *et al.*, Evaluation of novel carbamate insecticides for neurotoxicity to non-target species, *Pestic. Biochem. Physiol.*, 2013, **106**(3), 156–161.

31 D. R. Swale, P. R. Carlier, J. A. Hartsel, M. Ma and J. R. Bloomquist, Mosquitocidal carbamates with low toxicity to agricultural pests: an advantageous property for insecticide resistance management, *Pest Manage. Sci.*, 2015, **71**(8), 1158–1164.

32 WHO, Insecticide resistance, WHO, 2016 Sep 20, http://www.who.int/malaria/areas/vector_control/insecticide_resistance/en/.

33 J. A. Hartsel, D. M. Wong, J. M. Mutunga, M. Ma, T. D. Anderson, A. Wysinski, *et al.*, Re-engineering aryl methylcarbamates to confer high selectivity for inhibition of Anopheles gambiae versus human acetylcholinesterase, *Bioorg. Med. Chem. Lett.*, 2012, **22**(14), 4593–4598.

34 A. Ring, B. O. Strom, S. R. Turner, C. M. Timperley, M. Bird, A. C. Green, *et al.*, Bispyridinium Compounds Inhibit Both Muscle and Neuronal Nicotinic Acetylcholine Receptors in Human Cell Lines, *PLoS One*, 2015, **10**(8), e0135811.

35 V. Sepsova, J. Krusek, J. Zdarova Karasova, F. Zemek, K. Musilek, K. Kuca, *et al.*, The interaction of quaternary reversible acetylcholinesterase inhibitors with the nicotinic receptor, *Physiol. Res.*, 2014, **63**(6), 771–777.

36 E. Nepovimova, J. Korabecny, R. Dolezal, K. Babkova, A. Ondrejicek, D. Jun, *et al.*, Tacrine-Trolox Hybrids: A Novel Class of Centrally Active, Nonhepatotoxic Multi-Target-Directed Ligands Exerting Anticholinesterase and Antioxidant Activities with Low In Vivo Toxicity, *J. Med. Chem.*, 2015, **58**(22), 8985–9003.

37 J. Korabecny, R. Dolezal, P. Cabelova, A. Horova, E. Hruba, J. Ricny, *et al.*, 7-MEOTA-donepezil like compounds as cholinesterase inhibitors: Synthesis, pharmacological evaluation, molecular modeling and QSAR studies, *Eur. J. Med. Chem.*, 2014, **82**, 426–438.

38 J. Korabecny, M. Andrs, E. Nepovimova, R. Dolezal, K. Babkova, A. Horova, *et al.*, 7-Methoxytacrine-p-Anisidine Hybrids as Novel Dual Binding Site Acetylcholinesterase Inhibitors for Alzheimer's Disease Treatment, *Molecules*, 2015, **20**(12), 22084–22101.

39 S. K. Lee, M. K. Park, H. E. Jhang, J. Yi, K. Nahm, D. W. Cho, *et al.*, Preparation of 7-Methoxy Tacrine Dimer Analogs and Their In vitro/In silico Evaluation as Potential Cholinesterase Inhibitors, *Bull. Korean Chem. Soc.*, 2015, **36**(6), 1654–1660.

40 J. Cheung, M. J. Rudolph, F. Burshteyn, M. S. Cassidy, E. N. Gary, J. Love, *et al.*, Structures of human acetylcholinesterase in complex with pharmacologically important ligands, *J. Med. Chem.*, 2012, **55**(22), 10282–10286.

41 M. Harel, G. Kryger, T. L. Rosenberry, W. D. Mallender, T. Lewis, R. J. Fletcher, *et al.*, Three-dimensional structures of Drosophila melanogaster acetylcholinesterase and of its complexes with two potent inhibitors, *Protein Sci.*, 2000, **9**(6), 1063–1072.

42 J. Korabecny, L. Janovec, K. Musilek, F. Zemek, A. Horova, E. Nepovimova, *et al.*, Comparison of Novel Tacrine and 7-

MEOTA Derivatives with Aromatic and Alicyclic Residues: Synthesis, Biological Evaluation and Docking Studies, *Lett. Org. Chem.*, 2013, **10**(4), 291–297.

43 K. Musilek, O. Holas, J. Misik, M. Pohanka, L. Novotny, V. Dohnal, *et al.*, Monooxime-monocarbamoyl Bispyridinium Xylene-Linked Reactivators of Acetylcholinesterase-Synthesis, In vitro and Toxicity Evaluation, and Docking Studies, *ChemMedChem*, 2010, **5**(2), 247–254.

44 J. D. Durrant and J. A. McCammon, Molecular dynamics simulations and drug discovery, *BMC Biol.*, 2011, **9**, 71.

45 E. Paquet and H. L. Viktor, Molecular dynamics, monte carlo simulations, and langevin dynamics: a computational review, *BioMed Res. Int.*, 2015, **2015**, 183918.